Tanzania Journal of Engineering and Technology 2023, **42**(**4**):95-107
OPEN ACCESS articles distributed under Creative Commons Attribution Licence [CC BY-ND]
Websites: https://ajol.org/tjet; https://tjet.udsm.ac.tz

ISSN 1821-536X (**print**); ISSN 2619-8789 (**electronic**)
https://doi.org/ 10.52339/tjet.v42i4.958

Regular Research Manuscript

Augmented Finite Control Set MPC Design Technique for Wide Speed Range Control of Permanent Magnet Synchronous Motor Drives

Patrick Pilla, Francis Mwasilu†, and Emanuel Matee

Deparment of Electrical Engineering, University of Dar es Salaam, Tanzania.

†Corresponding author: fmwasilu@ieee.org

ORCID: https://orcid.org/0000-0001-7540-4198

ABSTRACT

The effective motion control task is highly influencing the final drive performance in wide-range motor drives applications such as electric vehicles (EVs), washing machines, compressors, elevators and lathe machines. Recently, permanent magnet synchronous motor (PMSM) drive has been widely employed in these applications to achieve desired performances such as high efficiency, high torque requirements with minimum size "occupancy". The PMSM drive features combining with these modern drive applications are highly nonlinear and the desired operation requirements demand high-performance control schemes with fast system response and robustness features. Linear control schemes are usually implemented to drive the PMSM that entail trade-offs between drive performance and simplicity in control implementation. Therefore, this paper presents the nonlinear control technique based on augmented finite control set (AFCS) model predictive control (MPC) scheme (AFCS-MPC). The proposed AFCS-MPC scheme enhances the standard MPC design by augmenting the nonlinear characteristics of the PMSM drive to achieve wide speed range drive performance under both steady-state and dynamic operating conditions. Comparative performance studies have been conducted and presented to confirm the efficacy of the proposed scheme.

ARTICLE INFO

Submitted: **Aug. 22, 2023**

Revised: **Dec. 27, 2023**

Accepted: **Jan. 15, 2024**

Published: **Feb., 2024**

Keywords: *Augmented Finite Control Set (AFCS), Field Oriented Control (FOC), Model Predictive Control (MPC), Permanent Magnet Synchronous Motors (PMSM).*

INTRODUCTION

Variable speed motor drives are widely used in industrial applications such as turning machine, robotics and CNC machine and electric submersible pump in subsea applications. In the past years, the DC motor drives and squirrel-cage induction motors (IMs) were the mostly accepted electric motors in industrial applications due to their attractive features they owned (Brinner *et al*., 2014; Da Cunha *et al*., 2018; Sul, 2011). Despite of their traits they are faced with inferior efficiency problem and poorer power factor (Pellegrino *et al*., 2012). Recently, the appealing features of the permanent magnet synchronous motor (PMSM) have prevailed and make it more attractive option in the modern industrial motor drive applications such as electric vehicles, railway trains (Calleja *et al*., 2016; Mwasilu, 2020), compressors(J. Kim et al., 2015), washing machines (Chi *et al*., 2009;

Jin *et al*., 2009). These salient features possessed by the PMSM drives are high efficiency, small weight-to-size ratio, wide speed range and good power factor to name a few (Leu *et al*., 2014; W. Wang *et al*., 2021).

Traditionally, the vector control based on proportional-plus integral plus derivative (PID) controller is a standard control scheme for both PMSM and IM motor drive applications (L. Wang *et al*., 2015). However, the PID control performance considering inherent drive nonlinear effects and robustness features requirements while guaranteeing the precise reference tracking capability are very poor. This is due to the fact that it is designed to control plant effectively and efficiently under the linear operating range. On the other hand, with the plant model exhibiting nonlinear features, the linear control schemes such as PID are to be replaced with the nonlinear control schemes to assure high performance results (De Soricellis *et al*., 2018; You & Kim, 2023; P. Zhang *et al*., 2022). Among numerous nonlinear control schemes such as sliding mode control, neural network control and Takagi-Sugeno fuzzy logic control; model predictive control (MPC) has emerged as impeccable options lately for motion control task since several constraints can be added in the MPC formulation to significantly enhance drive performance and overcome the PMSM nonlinearities (Rodriguez & Cortes, 2012). This peculiarity makes the MPC scheme being one of the best nonlinear control schemes for the PMSM drives when compared to the conventional PID or other nonlinear control architectures (Y. Zhang *et al*., 2017). The basic principle of the MPC is based on the use the current system model states to anticipate the future behavior of the state variables within a predefined control horizon in time. Thereafter, the selection of the optimal actuating control signal is determined by minimizing a pre-formulated cost function (Favato *et al*., 2021). The MPC formulation can be accomplished with continuous control set (CSS) or finite control set (FCS) contexts (Li *et al*., 2022). Different formulation and their comparative performance are reported in (Carlet et al., 2022; Turker *et al*., 2016; Xu *et al*., 2022). The FCS MPC is the main focus of this paper and for the sake of brevity more details are confined in this type of the MPC formulation. Despite of several advantages of the conventional FCS MPC control schemes as depicted in (Rodriguez & Cortes, 2012; L. Wang *et al*., 2015), they still face numerous challenges such as robustness against parameter variations (Yu *et al*., 2021) and persistent steady state errors between the reference signals and predictive signals. It is noted that the conventional FCS MPC scheme is characterised by high proportional gain that can result in finite steady state error (L. Wang *et al*., 2015). Therefore, it is difficult to guarantee at least near or zero steady state error with FCS MPC. This results into the high-performance features loss and unsuitable for some high precision control tasks. Several researches have been reported to overcome this control performance deficiency (Bolognani *et al*., 2009). To overcome this steady state error, the integral action inspired by the proportional plus integral scheme is employed in the MPC to formulate an augmented finite control set (AFCS) model predictive control (MPC) scheme.

In this paper, the augmented finite control set MPC scheme is proposed to enhance high control performances of the PMSM drives such as faster speed transient response and excellent reference tracking capabilities over a wide speed range covering constant torque region (Preindl & Bolognani, 2013a) and constant power or flux weakening region(Preindl & Bolognani, 2013b) when compared to the conventional linear PI speed controller. The salient performance features of the AFCS-MPC are validated through the comparative simulation results using MATLAB/Simulink platform.

DYNAMIC MODEL AND CURRENT LOOP CONTROL

Modelling of Permanent Magnet Synchronous Motor

The equivalent Permanent Magnet Synchronous Motor (PMSM) model based on the *d*-*q* axis, which rotate synchronously with angular velocity ω_r is given in state space form equation as in (1).

$$\frac{dx}{dt} = f(x,u),$$

$$x = \begin{bmatrix} i_{sd}^{\omega} & i_{sq}^{\omega} \end{bmatrix}^T, u = \begin{bmatrix} v_{sd}^{\omega} & v_{sq}^{\omega} \end{bmatrix}^T$$

$$f(x,u) = \begin{bmatrix} -1/\lambda_s\, i_{sd}^{\omega} + \omega_r i_{sq}^{\omega} + 1/L_s\, v_{sd}^{\omega} \\ -1/\lambda_s\, i_{sq}^{\omega} - \omega_r i_{sd}^{\omega} - \lambda_m/L_s\, \omega_r + 1/L_s\, v_{sd}^{\omega} \end{bmatrix} \quad (1)$$

$\lambda_s = L_s/R_s$ is the stator time constant; $i_{sd}^{\omega}, i_{sq}^{\omega}$ are components of the armature currents in *d*-axis and *q*-axis, respectively; R_s is stator resistance; $v_{sd}^{\omega}, v_{sq}^{\omega}$ are components of terminal voltage in *d*-axis and *q*-axis, respectively, L_s is the stator self-inductance in *d*-axis and *q*-axis, respectively; ω_r is synchronous rotor angular speed, λ_m is the magnetic flux linkage.

Theoretical Investigation of State-Steady Performance Considering Salient Pole PMSM Over a Wide Speed Range

In a constant torque region where the speed varies from zero to base speed, the salient-pole PMSM is regulated to capitalize the maximum torque at minimum copper losses, since the torque supplied is directly proportional to the stator currents. The control objective in this region is confined to trace the stator current locus vector along *OT* as illustrated in Figure 1 below. Nonetheless, above rated speed (that is beyond *T*), the stator current limits the developed maximum torque capability and forcing the operating point to be off-maximum torque per ampere (MTPA) trajectory control. Consequently, the control will be imposed to track the boundary of the stator current constraints (i.e.., tracking the path defined by (*TFGH*) while bound to trace the maximum voltage constraint curve(Preindl & Bolognani, 2015).

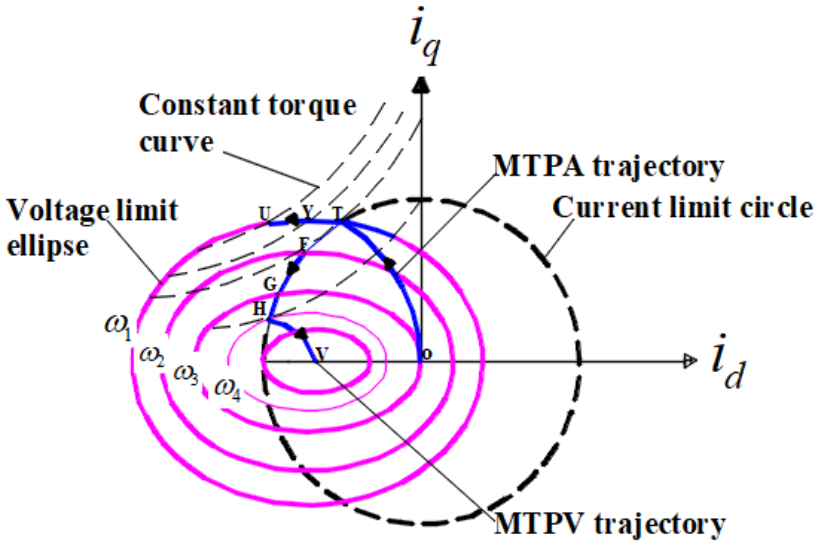

Figure 1: Stator current and voltage loci in *d*-*q* axis.

This happens when the PMSM drive rotor speed keeps on soaring further than the rated value. Taking into account that the rotor speed is fixed at the base speed outside *T*, with upsurge in torque requirement (as shown with *TYU* traces) the current vector violates the peak current limit constraint locus, which on the other

hand may cause saturation of the current control resulting in the lower torque generation (J.-M. Kim & Sul, 1997). Furthermore, the point formed by intersecting the individual voltage boundary and constant torque curves (i.e., showcased by *T*, *Y*, and *U*) turns to be the optimal points for achieving the least copper loss (Preindl & Bolognani, 2013a).The point of intersection between the respective voltage limit ellipses and the constant torque curves (i.e., illustrated by points *T*, *Y*, and *U*) becomes the optimum point in order to attain minimum copper loss (Sul, 2011).

Furthermore, as the rotor speed keep increasing beyond the rated speed along trajectory *FGH* the maximum torque should be minimized to accommodate the maximum voltage limit. The size of ellipse voltage constrains decrease as the speed increases. However, as the speed keeps on increasing, a point will be attained where additional upsurge will not guarantee the maximum voltage limit conditions of the salient-pole PMSM drive. Certainly, at point *H* with speed (ω_4) becomes the least speed for the control to comply with the voltage limit condition. Further to the point *Y*, the salient-pole PMSM drive control will be enforced to track the control trajectory along *HV* known as maximum torque per voltage (MTPV). Meaning that the speed control effort should always bound to the constant stator voltage or equivalent interpretation to this voltage. In this regard, the salient-pole PMSM drive speed control is accomplished from the least speed underneath base (ω_1) transiting through base speed to a very high deep speed above base at (ω_4) where a deep flux-weakening control regimes is comprehended by the trace of the MTPV trajectory (Preindl & Bolognani, 2013a, 2015). Further studies on wide speed range of PMSM from constant torque region to constant power region and even deep flux weakening regions can be found in (Bolognani et al., 2014; D. W. Kim et al., 2020; J.-M. Kim & Sul, 1997; Sue & Pan, 2008).

DISCRETE TIME MODEL AND FCS-MPC CONTROL DESIGN

FCS-MPC Control Design

FCS-MPC operate in discrete time. Consider the discrete time model as in state variable equation (1).

$$x_{(m+1)} = Ax_{(m)} + Bu_{(m)} \quad (2)$$

$$y_{(m)} = Cx_{(m)} + Du_{(m)} \quad (3)$$

where *x* is state variable and *u* is the system input while *y* is output and *A*, *B*, *C*, and *D* are parametric matrices representing plant model.

Considering the PMSM is fed by the two-level voltage source inverter (VSI), the FCS-MPC account for the switching combinations of six-semiconductor switches in the three legs of the VSI model. Thus, each control input inherits only two values, remaining the same during the sampling period, n , i.e., $S_i(t) \in \{0,1\}$, for all $t \in \left[mn,(m+1)n\right]$. Since, the input control belongs to finite number of switch combinations, such as, $S = \{S_1,.....,S_j\}$ where, S are switch states and j is the total number of switching combinations. In this case, there are eight switching combinations with respect to the input signals as shown in Figure 2 below.

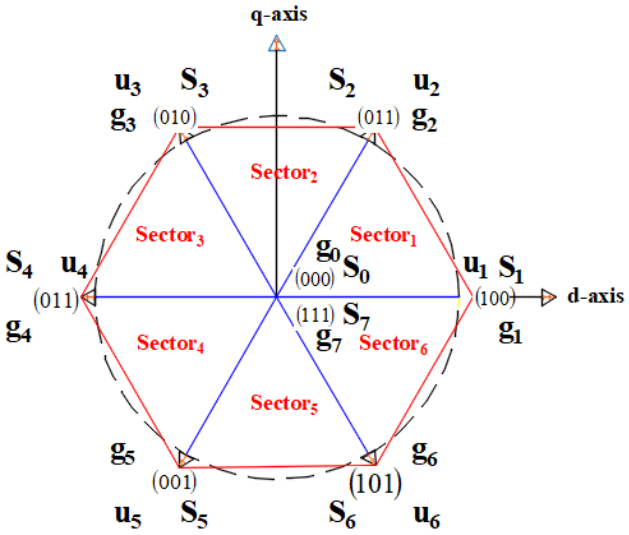

Figure 2: Control signals in the complex plane.

To predict the future behavior state of the system over a pre -determined horizon in time length J , the FCS-MPC employs a cost function, which considers the measurement until time m , future state and future actuation until the time $m+J$ as depicted in the Figure 3.

The cost function is given as,

$$g_{\vec{u}\in S}\left(x(m),\vec{u}\right) \qquad (5)$$

when $\vec{u}=\left\{u^{m},.....,u^{m+J-1}\right\}$ is feasible input sequence and $x(m)$ is a state variable.

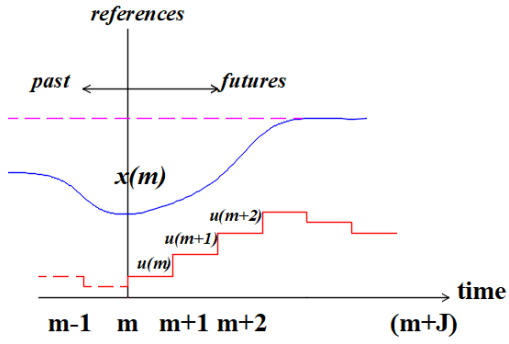

Figure 3: Illustration of FCS-MPC formulations.

Thus, the sequence of optimal actuation is selected by minimizing cost of function.

$$\vec{u}_{op}=\left\{u_{op}{}^{m}..,u_{op}{}^{m+J-1}\right\}\triangleq\left\{\min_{\vec{u}\in S} g\left(x(m),\vec{u}\right)\right\} \quad (4)$$

Cost function minimization is carried out by evaluating all available input signals. Finally, the controller applies only the first element in optimal actuation. $u^{m}\triangleq u_{op}^{m}$. Thus, this predictive technique directly provides the optimal actuation actions to control the drive and intermediate modulation stage is not required (Rodriguez & Cortes, 2012; L. Wang et al., 2015).

On implementation of FCS-MPC with pre-defined horizon in time J=1, there exist four main phases: Measurement, estimation, prediction and the optimal actuation. The scheme of these phases is illustrated in Figure 4, (Calleja et al., 2016).

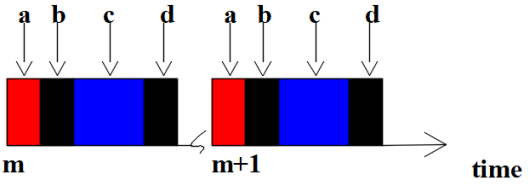

Figure 4. Execution scheme of the FCS-MPC for timing task.

Measurement: Since the building of model of prediction consider the discrete time, it is necessary to consider a measurement of the state variable, $x(m)$ at each sampling instant m .(in some cases, some of these variables can be estimated from other measurements). The measured state variables are applied by the controller to

select upon the optimal actuation to be used.

Estimation: To consider the calculation delays, in standard formulations, the optimal actuation is engaged at time $m+1$, u^{m+1}. Thus, the time delay of this action will be observed only at an instant $m+2$. This delay of one sampling period results the future reference variables to be calculated. This is achieved by taking the advantage of the fact that the previous optimal actuation, u^m , remain constant until the next sampling instant $m+1$. Therefore, the system model presented in (2), the system state, at an instant $m+1$can be estimated by:

$$x^{m+1} = f\left(x^m, u^m\right) \quad (5)$$

Prediction: In order to obtain the optimal actuation, FCS-MPC predicts the system behavior at the instant *m+2* by considering all available input signals at instant $m+1$. This is expressed through,

$$x^{m+2} = f\left(x^{m+1}, u^{m+1}\right) \quad (6)$$

These predictions are compared to the references by calculating the cost function $g^{m+1}(u_i)$,which is expressed in (7) below.

$$g^{m+1} = \left(x_r{}^{m+2} - x_p{}^{m+2}\right)^T W \left(x_r{}^{m+2} - x_p{}^{m+2}\right) \quad (7)$$

where *W* is representing a weighting matrix and x_r is signifying reference state variable. Thus, the optimal actuation $u^{m+1}$is that one which gives out the minimum value in the cost function.

Proposed AFCS-MPC Control Design

Finite control set MPC described in previously adopts the high feedback gain with inclusion of restrictions and constraints in their control. This results the existence of steady state error and poor disturbance rejection in some cases. To overcome this, the integral action is introduced to the FCS-MPC and the controller enumerated as augmented finite control set model predictive control scheme (AFCS-MPC). The main objective of the proposed AFCS-MPC is to achieve an optimal output of the feedback control by employing a gain matrix Z_{fcs}. The optimal control signals $u^{op}{}_{(m)}$ is written as equation (8),

$$\begin{bmatrix} u_1{}^{op}{}_{(m)} \\ u_2{}^{op}{}_{(m)} \end{bmatrix} = Z_{fcs}\left(\begin{bmatrix} x^r_{1(m)} \\ x^r_{2(m)} \end{bmatrix} - \begin{bmatrix} x^p_{1(m)} \\ x^p_{2(m)} \end{bmatrix}\right) \quad (8)$$

where Z_{fcs} stands for the feedback gain, x_r for the reference value and x the measured output response. The (Z_{fcs}) is obtained as depicted on (9) below

$$Z_{fcs} = B^{-1}A \quad (9)$$

The integral error signal from the reference state and measured state output response are added to the controller. An integrator in discrete-time system is expressed as $z_i \frac{1}{1-z^{-1}}$, where z^{-1} is the backward shift operator stands for $z^{-1}x_{(m)} = x_{(m-1)}$ .This term augment the conventional FCS-MPC to improve steady state performance. Therefore, the enhanced MPC form is expressed as in equation (10),

$$\begin{bmatrix} u_1{}^{op}{}_{(m)} \\ u_2{}^{op}{}_{(m)} \end{bmatrix} = Z_{fcs}\frac{Z_i}{1-z^{-1}}\left(\begin{bmatrix} x^r_{1(m)} \\ x^r_{2(m)} \end{bmatrix} - \begin{bmatrix} x^p_{1(m)} \\ x^p_{2(m)} \end{bmatrix}\right) - Z_{fcs}\begin{bmatrix} x^p_{1(m)} \\ x^p_{2(m)} \end{bmatrix} \quad (10)$$

where Z_i is the integral gain for the input signal with the value range of $0 < Z_i < 1$. The actual control input signal $u_{(m)}$ for the AFCS-MPC is obtained by evaluating the cost of function for all available control candidates. Therefore, the objective function in optimal solution of the one step ahead prediction algorithm is given as in equation (11) The scheme for this algorithm is clearly depicted in the Fig. 5.

$$g = \left(u_{1(m)} - u_1^{op}{}_{(m)}\right)^2 + \left(u_{2(m)} - u_2^{op}{}_{(m)}\right)^2 \quad (11)$$

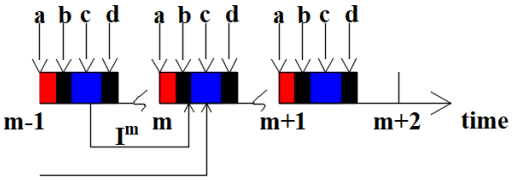

Figure 5. Execution sequence scheme of AFCS- MPC control design.

Figure 6. demonstrates the configuration that consists of inner-loop for the proportional control with gain of Z_{fcs} and outer loop for integral control with gain of Z_i. Inner loop provides the relationship between $u_{(m)}$ and $y_{(m)}$ while the integral controller design defines the closed-loop transfer function in (12).

$$y_{(m+1)} = Cx_{(m)} + Du_{(m)} \quad (12)$$

and the control input signal is provided in (13) as:

$$u_{(m)} = Z_{fcs}\left(g_{(m)} - y_{(m)}\right) \quad (13)$$

where $g_{(m)}$ is the control input signal of the outer loop and $u_{(m)}$ is the reference value of the inner loop system. The outer loop feedback system, which has an integral action, can be designed in a straightforward manner. The outer loop includes a function of integral action $Z_i \dfrac{1}{1-z^{-1}}$ and the time delay z^{-1} from the inner loop. Thus, the transfer function of outer loop system is expressed as:

$$\frac{Y_{(z)}}{G_{(z)}} = Z_i \frac{z^{-1}}{1 - z^{-1} + Z_i z^{-1}} \quad (14)$$

where the closed-loop pole is selected to be $1 - Z_i$. Selection of the closed loop pole lies in a range of $0 \le r_{cl} \le 1$ results to an integral gain $Z_{fcs} = 1 - r_{cl}$. The pole r_{cl} is a design parameter that is selected and pre-set. Thus, the position of the closed-loop pole can be adjusted depending on the desired time constant of the feedback system. $\triangle y = y_{(m)} - y_{(m-1)}$, integral gain results to the optimal actuation, which is $u^{op}{}_{(m)}$ and can be expressed as portrayed in equation (15) below,

$$u^{op}{}_{(m)} = u^{op}{}_{(m-1)} + Z_{fcs}\left(z_i(y^r{}_{(m)} - y^p{}_{(m)}\right) - Z_{fcs}(\triangle y_{(m)}) \quad (15)$$

where, y^r is the reference value and y^p is the measured output values.

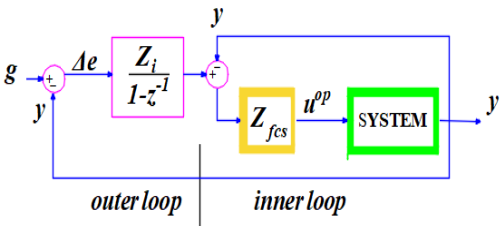

Figure 6: Schematic for the AFCS-MPC scheme.

Conventional Field-Oriented Control (FOC) Scheme Control Design

The FOC is linear control system, which is represented in transfer function $G(z)$ and the controller in $C(z)$.

There are four main variables in the control loop i.e., reference value R_z, control input U_z ,measured output Y_z and control error E_z .The transfer function in a first order ARX model is given as:

$$G_{(z)} = \frac{Y_{(z)}}{U_{(z)}} = \frac{b_1}{z + a_1} \quad (16)$$

Proportional control is applied when the control signal is subjected to the proportional with the change of error value $\Delta e = g_{(z)} - y_{(z)}$. Z_p and Z_{in} stands for the proportional gain and integral gain respectively. The transfer function for the proportional plus integral (PI) controller is expressed as in equation (17).

$$C_{(z)} = \frac{U_{(z)}}{E_{(z)}} = Z_p + \frac{Z_{in}}{1 - z^{-1}} = \frac{\left(Z_{in} + Z_p\right)z - Z_p}{z - 1}) \quad (17)$$

Controller gain (Z_{in} and Z_p) are obtained using pole placement method. Thus, the feedback control illustrated on Figure 7 is given as:

$$\frac{Y_{(z)}}{R_{(z)}} = \frac{C_{(z)}G_{(z)}}{1-C_{(z)}G_{(z)}} \quad (18)$$

The denominator polynomial is also known as characteristics equation of the control system. Therefore, the roots of this polynomial are equal to the desired closed-loop poles. If the polynomial function of the chosen closed loop is given as:

$$D_{\alpha\beta} = z^2 - (\alpha+\beta)z + \alpha\beta \quad (19)$$

The gains are derived by the equation depicted as:

$$Z_p = -\frac{(\alpha\beta + a_1)}{b_1} \quad (20)$$

$$Z_{in} = \frac{(\alpha+\beta)+1-a_1}{b_1} - Z_p \quad (21)$$

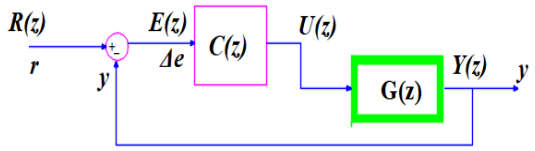

Figure 7: Schematic of the conventional FOC scheme.

PERFORMANCE ASSESSMENT

Scenario Setup and PMSM Drive Parameter Description

The simulations were conducted by using MATLAB/Simulink program. During the simulation studies, the fixed sampling interval of 40 μs was selected for the AFCS-MPC algorithmm. The gains parameters and bandwidths of the FOC control scheme for the speed and current loops are properly selected by using the pole placement technique, the gains based on the proportional plus integral (PI) controller are Z_{ps} = 0.0142 and Z_{ins} = 1.26 for the speed loop with a bandwidth of 20 Hz and Z_{pc} =314.16 and Z_{inc}=7489.556 for the current loop with the bandwidth set twenty times higher than the bandwidth of the speed loop to guarantee decoupling of the mechanical and electrical system dynamics . Similarly, the gains parameters and bandwidths of the speed outer loop the proposed AFCS-MPC and current loops are chosen appropriately based on the pole placement principle. The gains are Z_{ps} = 0.0142 and Z_{is}= 1.26 for the speed loop with a bandwidth of 20 Hz and Z_i= 0.2 for the current loop with bandwidths set twenty times higher than that of the speed loop. The two loops have been designed fairly similar to the conventional control scheme in order to retain their inherent performance characteristics. This guarantees that the comparative salient characteristics performance of the proposed scheme is not influenced by the tuning parameters.

Different scenarios have been selected to test the efficacy of the proposed scheme as described below. The first scenario, shows the demonstrate computer simulation of the PMSM motor drive whose parameters have been tabulated as depicted on Table 1 below. The motor drive is subjected to the multi-stepped rotor speed as follows (i.e., 800→1400→2000→1400 →800 r/min). Likewise, the second scenario shows the simulation of interior PMSM Motor drive subjected on the sudden load change with fast step as follows (i.e.,0.5→1.5→0.5 N·m) while the commanded speed established constant at 900 r/min. These scenarios set to reveal the rigorous transient response performance of the PMSM drive under the proposed scheme. Third scenario ascertain to demonstrate the simulation of the PMSM drive subjected to a low speed approximated at 100 r/min with parameter variations of 150% of q-axis inductance and 70% of magnetic flux linkage while the load torque is set constant at 1.5 N·m. This scenario set to reveal robustness performance features of the proposed scheme. The scenario mentioned above were carried out under a constant torque region. This is due to the fact that under speed condition below or equal to the base, the PMSM drive is expected to experience parameter change due to heavy load. If the

PMSM drive is operated at very high speed definitely the winding temperature increase and bearing friction and other nonlinear mechanical loading might be excited (D. W. Kim *et al.*, 2020). Capturing these unmodeled dynamics is not a trivial study and therefore their effects are out of the scope of the current paper. On the fourth scenario, the simulation of the PMSM drives under wide speed range with step change under constant torque region from 2000 r/min to 2500 r/min (rated speed) and constant power region (flux weakening region) from 2500 to 3000 r/min.

Table 1: Parameters of the PMSM Drives

Parameters	Symbol	Value	Unit
Stator resistance	R_s	3	Ω
Flux linkage	λ_m	0.125	Wb
Stair Inductance	L_s	7	mH
Pole Pairs	p	2	-
Moment of inertia	J	0.00001	kg.m^{-2}
Viscous damping	B_v	0.00011	Nm.s /rad
Sampling time	T_s	40	µs
DC bus voltage	V_{DC}	300	V
Rated Torque	T	1.5	Nm
Rated speed	ω_{rated}	2500	rpm

PERFORMANCE ASSESSMENT WITH SIMULATION RESULTS

In the first scenario: The PMSM drive with stepped rotor speed starting from 800 r/min rises up to a constant speed of 1400 r/min and again stepped to the speed of 2000 r/min and afterward, it is changed downward stepwise in a mirror image of the first setup as shown on the Figs. 8 and 9. The simulation results which are displayed on the Figure 8 and Figure 9 demonstrate the comparative study of the conventional FOC and proposed AFCS-MPC schemes, respectively. The results of the proposed AFCS-MPC give fast speed response with steady state error approximate less than 0.49 r/min from the commanded speed in a constant torque region. Also, the PMSM drive has proven to deliver an excellent torque response under this speed change scenario. In the second scenario: the drive with the load torque T_L change in step from 0.5 to 1.5 N·m at 0.2 s which followed with mirror image of the first step change at 0.8 s as given in the Figure 8.

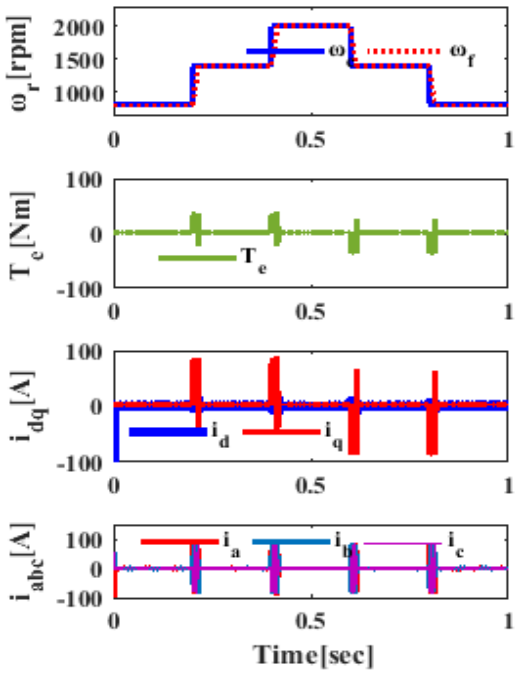

Figure 8: Simulation results for conventional FOC scheme under first scenario.

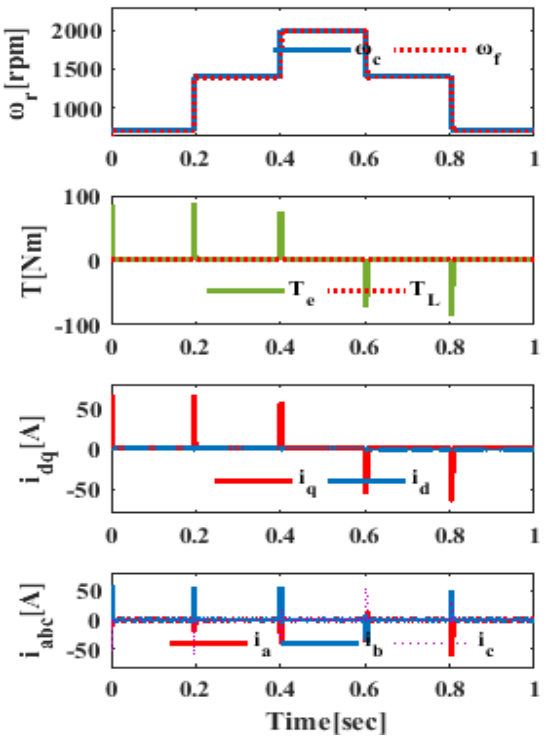

Figure 9: Simulation results for the proposed AFCS-MPC scheme under first scenario.

The results on Figure 10 and Figure 11 also demonstrates the comparative study of the conventional FOC and proposed AFCS-MPC control schemes, respectively. It is clearly seen that the AFCS-MPC scheme gives the smaller steady state error (i.e., less than 0.5 r/min), which implies that despite of the existing nonlinearities of the PMSM drive, speed response has no significant oscillation and little overshoot over the entire operating constant regions. Furthermore, in third scenario: the PMSM drive with parameter variations subjected under low speed (100 r/min) while the load torque (T_L) is maintained at 1.5 N·m as shown on Figure 12 and Figure 13. These results demonstrate the comparative study of the conventional FOC and proposed AFCS-MPC control scheme, respectively. These results confirm that with AFCS-MPC control scheme, the steady state speed error is almost negligible compared to the error found on the conventional FOC control scheme (i.e.,15 r/min). In the fourth scenario: the drive with speed step change covers the wide speed range as shown in the Figure 14 The result confirms the PMSM drive is fully controlled by using the proposed AFCS-MPC control scheme in the constant torque region and flux weakening region as well with negligible steady state errors.

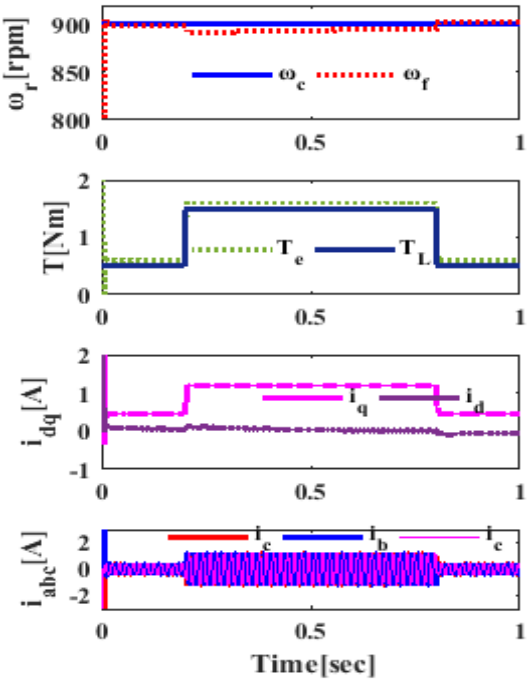

Figure 10: Simulation results for conventional FOC scheme under second scenario.

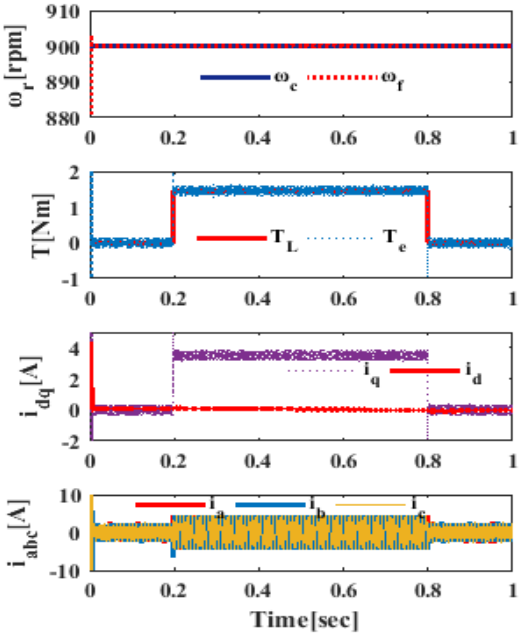

Figure 11: Simulation results for the proposed AFCS-MPC scheme under second scenario.

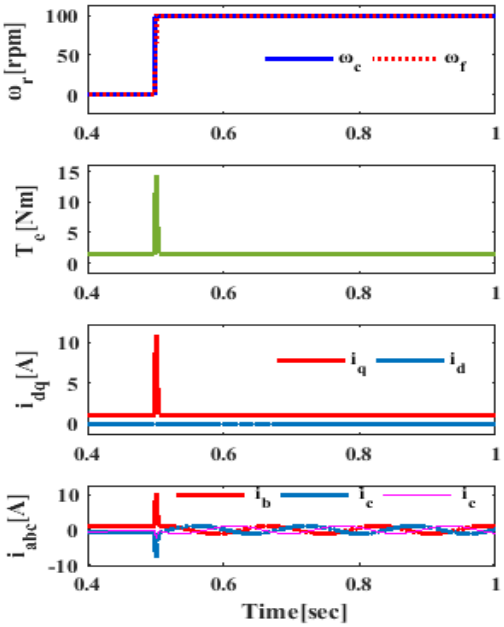

Figure 13: Simulation results for the proposed AFCS-MPC scheme under third scenario.

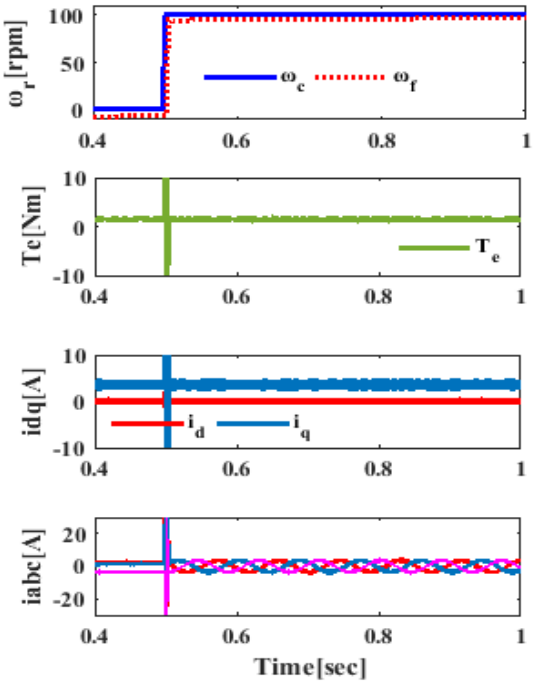

Figure 12: Simulation results for the conventional FOC scheme under third scenario

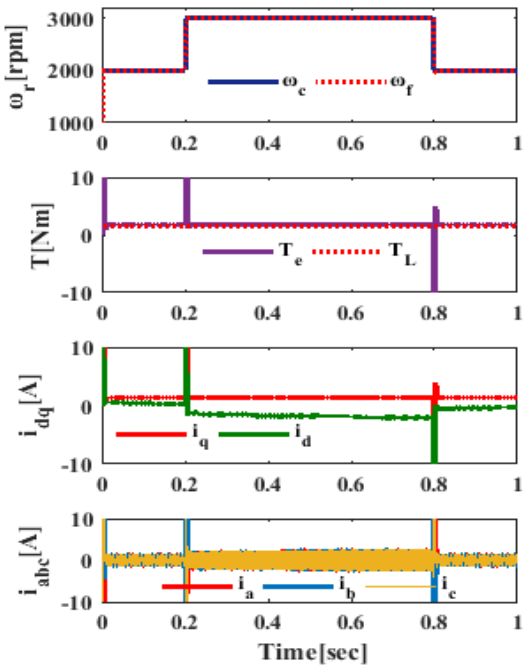

Figure 14: Simulation results for the proposed AFCS-MPC scheme under fourth scenario.

CONCLUSIONS

This paper has presented the AFCS-MPC scheme that was implemented and evaluated based on the PMSM drive. The performance evaluation has been assessed by using computer simulation results obtained from the MATLAB/Simulink platform. The proposed AFCS-MPC scheme has demonstrated the high precision performance under various conditions in both constant torque and constant power regions. In both regions, the proposed AFCS-MPC has demonstrated fast transient response and the better speed response as can be observed in the simulation results.

This study suggests the following future research work for further performance improvement of the PMSM drive. This work studied the analysis of the PMSMs under constant power region that is carried out on lossless equivalent circuit model of the PMSM under theoretical steady state characteristics. However, when the motor core losses are not taken into account, this tends to limit the inverter to utilize the

maximum dc link available voltage, specifically at high speed in flux weakening region. There is a strong effect exploited by motor core loss on the time harmonics of magnetic flux density. Therefore, a mathematical model to deduce the motor core loss is mandatory for the precision prediction of the power capability of the PMSM over a wide speed range. This study will be reported in our future work.

REFERENCES

Bolognani, S., Bologani, S., Peretti, L., & Zigliotto, M. (2009). Design and implementation of model predictive control for electrical motor drives. *IEEE Transactions on Industrial Electronics*, **56**(6), 1925–1936. https://doi.org/10.1109/TIE.2008.2007547

Bolognani, S., Calligaro, S., & Petrella, R. (2014). Adaptive Flux-Weakening Controller for Interior Permanent Magnet Synchronous Motor Drives. *IEEE Journal of Emerging and Selected Topics in Power Electronics*, **2**(2), 236–248. https://doi.org/10.1109/JESTPE.2014.2299153

Brinner, T. R., McCoy, R. H., & Kopecky, T. (2014). Induction versus permanent-magnet motors for electric submersible pump field and laboratory comparisons. *IEEE Transactions on Industry Applications*, **50**(1), 174–181. https://doi.org/10.1109/TIA.2013.2288203

Calleja, C., Lopez-De-Heredia, A., Gaztanaga, H., Aldasoro, L., & Nieva, T. (2016). Validation of a Modified Direct-Self-Control Strategy for PMSM in Railway-Traction Applications. *IEEE Transactions on Industrial Electronics*, **63**(8), 5143–5155. https://doi.org/10.1109/TIE.2016.2572661

Carlet, P. G., Favato, A., Bolognani, S., & Dorfler, F. (2022). Data-Driven Continuous-Set Predictive Current Control for Synchronous Motor Drives. *IEEE Transactions on Power Electronics*, **37**(6), 6637–6646. https://doi.org/10.1109/TPEL.2022.3142244

Chi, S., Zhang, Z., & Xu, L. (2009). Sliding-mode sensorless control of direct-drive PM synchronous motors for washing machine applications. *IEEE Transactions on Industry Applications*, **45**(2), 582–590. https://doi.org/10.1109/TIA.2009.2013545

Da Cunha, G., Rossa, A. J., Alves, J. A., & Cardoso, E. (2018). Control of Permanent Magnet Synchronous Machines for Subsea Applications. *IEEE Transactions on Industry Applications*, **54**(2), 1899–1905. https://doi.org/10.1109/TIA.2017.2785764

De Soricellis, M., Da Rù, D., & Bolognani, S. (2018). A Robust Current Control Based on Proportional-Integral Observers for Permanent Magnet Synchronous Machines. *IEEE Transactions on Industry Applications*, **54**(2), 1437–1447. https://doi.org/10.1109/TIA.2017.2772171

Favato, A., Carlet, P. G., Toso, F., Torchio, R., & Bolognani, S. (2021). Integral Model Predictive Current Control for Synchronous Motor Drives. *IEEE Transactions on Power Electronics*, **36**(11), 13293–13303. https://doi.org/10.1109/TPEL.2021.3081827

Jin, C. S., Jung, D. S., Kim, K. C., Chun, Y. Do, Lee, H. W., & Lee, J. (2009). A study on improvement magnetic torque characteristics of IPMSM for direct drive washing machine. *IEEE Transactions on Magnetics*, **45**(6), 2811–2814. https://doi.org/10.1109/TMAG.2009.2018667

Kim, D. W., Kang, D. H., Kim, C. H., Kim, J. S., Kim, Y. J., & Jung, S. Y. (2020). Operation Characteristic of IPMSM Considering PM Saturation Temperature. *IEEE Transactions on Applied Superconductivity*, **30**(4). https://doi.org/10.1109/TASC.2020.2989799

Kim, J., Jeong, I., Nam, K., Yang, J., & Hwang, T. (2015). Sensorless control of PMSM in a high-speed region considering iron loss. *IEEE Transactions on Industrial Electronics*, **62**(10), 6151–6159.

https://doi.org/10.1109/TIE.2015.2432104

Kim, J.-M., & Sul, S.-K. (1997). Speed Control of Interior Permanent Magnet Synchronous Motor Drive for the Flux Weakening Operation. *IEEE Transactions on Industry Applications*, **33**(1), 43–48.

Leu, V. Q., Mwasilu, F., Choi, H. H., Lee, J., & Jung, J. W. (2014). Robust fuzzy neural network sliding mode control scheme for IPMSM drives. *International Journal of Electronics*, **101**(7), 919–938. https://doi.org/10.1080/00207217.2013.805359

Li, X., Tian, W., Gao, X., Yang, Q., & Kennel, R. (2022). A Generalized Observer-Based Robust Predictive Current Control Strategy for PMSM Drive System. *IEEE Transactions on Industrial Electronics*, **69**(2), 1322–1332. https://doi.org/10.1109/TIE.2021.3062271

Mwasilu, F. (2020). Direct predictive speed control of salient PMSM drives in constant. *Tanzania Journal of Engineering and Technology*, **39**(2), 127–143.

Pellegrino, G., Vagati, A., Boazzo, B., & Guglielmi, P. (2012). Comparison of induction and PM synchronous motor drives for EV application including design examples. *IEEE Transactions on Industry Applications*, **48**(6), 2322–2332. https://doi.org/10.1109/TIA.2012.2227092

Preindl, M., & Bolognani, S. (2013a). Model predictive direct torque control with finite control set for PMSM drive systems, Part 1: Maximum torque per ampere operation. *IEEE Transactions on Industrial Informatics*, **9**(4), 1912–1921. https://doi.org/10.1109/TII.2012.2227265

Preindl, M., & Bolognani, S. (2013b). Model predictive direct torque control with finite control set for pmsm drive systems, part 2: Field weakening operation. *IEEE Transactions on Industrial Informatics*, **9**(2), 648–657. https://doi.org/10.1109/TII.2012.2220353

Preindl, M., & Bolognani, S. (2015). Optimal State Reference Computation with Constrained MTPA Criterion for PM Motor Drives. *IEEE Transactions on Power Electronics*, **30**(8), 4524–4535. https://doi.org/10.1109/TPEL.2014.2354299

Rodriguez, J., & Cortes, P. (2012). *Predictive Control of Power Converters and Electrical Drives*. University Press of Mississippi for the Southern Quarterly.

Sue, S. M., & Pan, C. T. (2008). Voltage-constraint-tracking-based field-weakening control of IPM synchronous motor drives. *IEEE Transactions on Industrial Electronics*, **55**(1), 340–347. https://doi.org/10.1109/TIE.2007.909087

Sul, S. K. (2011). *Control of Electric Machine Drive Systems*. IEEE Press-Wiley.

Turker, T., Buyukkeles, U., & Bakan, A. F. (2016). A Robust Predictive Current Controller for PMSM Drives. *IEEE Transactions on Industrial Electronics*, **63**(6), 3906–3914. https://doi.org/10.1109/TIE.2016.2521338

Wang, L., Chai, S., Yoo, D., Gan, L., & Ng, K. (2015). *PID AND Predictive Control of Electrical Drives and Power Converters Using MATLAB ® /Simulink ®*. IEEE-Wiley.

Wang, W., Du, M., & Wei, K. (2021). Rapid Torque Rising of PMSM by Directly Chasing Rotating Flux Linkage Vector. *IEEE Journal of Emerging and Selected Topics in Power Electronics*, **9**(4), 4384–4394. https://doi.org/10.1109/JESTPE.2020.3048091

Xu, S., Sun, Z., Yao, C., Zhang, H., Hua, W., & Ma, G. (2022). Model Predictive Control With Constant Switching Frequency for Three-Level T-Type Inverter-Fed PMSM Drives. *IEEE Transactions on Industrial Electronics*, **69**(9), 8839–8850. https://doi.org/10.1109/TIE.2021.3114716

You, S., & Kim, W. (2023). Adaptive Learning Gain-Based Control for Nonlinear Systems With External Disturbances: Application to PMSM. *IEEE Transactions on Control Systems Technology*, **31**(3), 1427–1434. https://doi.org/10.1109/TCST.2022.3208446

Yu, F., Zhou, C., Liu, X., & Zhu, C. (2021). Model-Free Predictive Current Control for Three-Level Inverter-Fed IPMSM with an Improved Current Difference Updating Technique. *IEEE Transactions on Energy Conversion*, **36**(4), 3334–3343. https://doi.org/10.1109/TEC.2021.3069274

Zhang, P., Chen, Y., Wan, Z., & Zhang, W. (2022). Adaptive Finite-Time Backstepping Sliding Mode Control for PMSM System With Backlash. *IEEE Journal of Emerging and Selected Topics in Power Electronics*, **10**(6), 7549–7559. https://doi.org/10.1109/JESTPE.2022.3183263

Zhang, Y., Xia, B., & Yang, H. (2017). Performance evaluation of an improved model predictive control with field-oriented control as a benchmark. *IET Electric Power Applications*, **11**(5), 677–687. https://doi.org/10.1049/iet-epa.2015.0614

.